# Diffusion coefficients of supercritical carbon dioxide and its mixtures using molecular dynamic simulations

**Ji-Hyun Yoo\*, Alexander Breitholz\*, Yoshio Iwai\*\*, and Ki-Pung Yoo\*,†**

\*Department of Chemical and Biomolecular Engineering, Sogang University, Seoul 121-742, Korea
\*\*Department of Chemical Systems and Engineering, Kyushu University, Fukuoka 812-8581, Japan

**Abstract**–Molecular dynamic simulations have been evaluated for systems containing supercritical carbon dioxide to predict high-pressure diffusion coefficients of binary mixtures. Diffusion coefficients of high boiling compounds in supercritical fluids are important for the design of supercritical extractors, separators and reactors. Since high-pressure experiments are time intensive and difficult to perform, molecular simulations could prove a useful framework to obtain thermodynamic properties; however, their reliability is still in question. In this work, an NVT ensemble single site model molecular dynamic simulation using gear predictor corrector algorithm has been applied to calculate diffusion coefficients of carbon dioxide, naphthalene, 2,6-dimethylnaphthalene and 2,7-dimethylnaphthalene in supercritical carbon dioxide system at 317.5 K. The Lennard-Jones (12-6) and the Coulomb potential function have been combined into an intermolecular potential function to measure the binary molecular interaction. The simulation results of the diffusion coefficients are being compared with similar experimental data near the critical points. The calculated diffusion coefficients for each system behaved as a monotonic decreasing function of the molar density and the molecular simulations results, and the selected experimental data are in good agreement.

Key words: Supercritical Carbon Dioxide, Molecular Dynamic Simulations, Diffusion Coefficients

## INTRODUCTION

Research and applications in the field of supercritical fluids (SCFs) have increased due to their unique properties like high diffusivity, low viscosity, and adjustable solvency power. The supercritical fluids region is defined as a part of PVT surface which is located above the critical point except near critical and extremely high-pressure regions [1]. Recent research is focused on the prediction of fundamental property values needed for design and understanding of the molecular interactions for physicochemical process such as SCFs system that have been widely used as solvents in chemical reactions, extraction and adsorption processes [2-4].

Diffusion coefficients of high boiling compounds in supercritical fluids are needed for the design of supercritical extractors, separators and reactors. Since it is necessary to ascertain the values of the mass transfer parameters of the system in the modeling and subsequent design of industrial processes, recent research is expanding the database for binary diffusion coefficients and exploring the influence on solute diffusivities the addition of a second component to the process fluid [5-8].

However, compared to other transport properties, experimental data on diffusion coefficients are scarce because of the technical difficulties of these measurements [9]. In the traditional sense, predictive equations for diffusion in liquids or gases are not applicable in the supercritical region, and high-pressure experiments are time intensive and difficult to perform; thus molecular dynamic (MD) simulation could prove a useful tool to obtain thermodynamic properties [10].

Usually, computer simulation methods have been used to investigate structural and thermodynamic properties, and other useful information that is hardly obtained by experiment [11]. During the last decades MD simulation techniques have opened avenues in the estimation and prevision of thermo-physical properties (both under equilibrium and non-equilibrium conditions) of simple molecular fluids [12]. Despite MD simulation only being applied for a narrow range of molecular weight ratios, molecular diameter ratios, and densities and the limitations imposed by the computing resources currently available, simulations can still be considered cheaper and faster than real experiments, at least for simple molecules [10].

In previous works [13,14], the Lennard-Jones potential function has been adopted for intermolecular potential to calculate the diffusion coefficient of supercritical carbon dioxide and aromatic hydrocarbon systems. In this work, the Lennard-Jones (12-6) and the Coulomb potential function have been combined to an intermolecular potential function to measure the interaction between pairs of molecules.

An NVT ensemble single site model MD simulation with the Lennard-Jones (12-6) and the Coulomb potential function has been applied to calculate the self diffusion coefficients of carbon dioxide and diffusion coefficients of naphthalene, 2,6-dimethylnaphthalene, and 2,7-dimethylnaphthalene in supercritical carbon dioxide system at 317.5 K. The simulation results of the diffusion coefficients are compared with the experimental data [15,16] near the critical points.

## THEORY

### 1. Potential Function and Parameters

The accuracy of predictions by molecular simulation strongly depends on the intermolecular potential involved, and the determi-

---

†To whom correspondence should be addressed.
E-mail: kpyoo@sogang.ac.kr

nation of a suitable potential has also proved to be a considerable challenge [17]. A good potential should be accurate, simple in form and more importantly transferrable, which means that it can be easily used to study systems. For the above reasons, in this study molecular dynamics simulation has been performed with the TraPPE-UA force field and elementary physical model (EPM2) model [18]. The TraPPE-UA force field model is adopted due to accuracy and simplicity in forms, which means that it can be easily used to study both single-component and multi-component systems. The EPM2 potential is selected due to its simplicity and it has been proven suitable for simulations of simple mixtures, and EPM2 carbon dioxide uses partially charged Lennard-Jones beads for modeling the carbon atom as well as for representing the two oxygen atoms [19]. It is widely believed that the carbon dioxide molecule is very stable with a linear geometry. However, some investigations regarding supercritical $CO_2$ (SCCO2) have shown that its structure has a marginal deviation from linear geometry [11].

To account for this deviation, the EPM2 potential is used to describe supercritical carbon dioxide, naphthalene, 2,6-dimethylnaphthalene, and 2,7-dimethylnaphthalene. This bonded potential molecule consists of rigid bonds and a flexible bond angle potential. The non-bonded and charged interactions are between atoms belonging to different molecules. Carbon dioxide was treated as a single-site molecule, and aromatic compounds were treated as multisite molecules. For aromatic compounds, a benzene ring, a methyl group and a hydroxyl group were adopted for unlike pair states [20,21]. In this work, the software Gaussian R03W, version 6.0 has been adopted to check the value of the molecular weight, coordination, connectivity, length, and degree of structural angle.

For the non-bonded van der Waals interactions, the Lennard-Jones (12-6) and the Coulomb potential function have been combined into an intermolecular potential function to measure the interaction between a pair of molecules,

$$\emptyset(r_{ij}) = 4\varepsilon_{ij}\left[\left(\frac{\sigma_{ij}}{r_{ij}}\right)^{12} - \left(\frac{\sigma_{ij}}{r_{ij}}\right)^6\right] + \frac{q_i q_j}{4\pi\varepsilon_0 r_{ij}} \tag{1}$$

where $\emptyset$ is the intermolecular potential, $\varepsilon$ is the energy parameter, $\sigma$ is the size parameter, r is the molecular distance, q is the charge parameter and i and j denote the particles i and j, respectively. The intermolecular potential parameters and partial charges carried by each group are listed in Table 1.

For interactions between groups of like molecules, pure component parameters had been determined using the Lorentz-Berthelot combining rules in the case of calculating Lennard-Jones parame-

ters to study binary liquids mixtures,

$$\sigma_{ij} = (1 - l_{ij})\frac{(\sigma_{ii} + \sigma_{jj})}{2} \tag{2}$$

$$\varepsilon_{ij} = (1 - k_{ij})\sqrt{\varepsilon_{ii}\varepsilon_{jj}} \tag{3}$$

where $l_{ij}$ and $k_{ij}$ are the intermolecular interaction parameters between unlike molecules.

The Lorentz-Berthelot rules estimate the intermolecular potential parameters for a mixed pair of molecules (ij where i≠j) by combining the analogous potential parameters for the two pairs of identical molecules (ii and jj). These relations allow the calculation of the solubility of high-boiling compounds in SCCO2 [23-25].

The Lennard-Jones (L-J) (12-6) potential function has been expressed by the van der Waals energy corresponding repulsion and attraction which creates temporarily induced dipole moment occurring by the motion of electrons and describes effectively the interaction between two uncharged molecules or atoms. In L-J (12-6) potential function, the $r^{-12}$ term describes Pauli repulsion at short ranges due to overlapping electron orbitals, and the $r^{-6}$ term describes attraction at long ranges that is called van der Waals force. The L-J (12-6) potential function has simply explained the properties of gases, particularly accurate for gas, and to model dispersion and overlap interactions in molecular models [26].

The Coulomb potential function describes the interactions between molecules due to their permanent dipole moments that attract and repel one another. The Coulomb interaction energy between two molecules in a van der Waals complex has been computed by summing the additive atom-atom contributions between the molecules [27].

## 2. Einstein Function

To get diffusion coefficients, the Einstein equation has been used for the center of mass of the solute molecules,

$$L_{MSD} = \frac{1}{N}\Sigma_N^i|r_i(t) - r_i(t_0)|^2 \tag{4}$$

$$D = \frac{1}{6\Delta t}L_{MSD} \tag{5}$$

where t is the elapsed time, r is the position of a particle for each component and N is the number of molecules. The diffusion coefficients D were determined from the Einstein relation as the mean-square displacement along the unfolded trajectory of a tracer particle [28].

To determine the long time limit of the slope of a mean squared displacement function, it is plotted over time in a so-called Einstein plot. The long time limit of the slope is then obtained from a least squares fit of a straight line to the linear regime of the plot. From the derivation of the generalized Einstein relations, it is known that the mean squared displacement, its corresponding time correlation function and the derivative of the mean squared displacement with respect to time are closely related to each other by simple mathematical operations. From the relationships between the functions it is evident that the slope is obtained by the fit of a straight line to the mean squared displacement. This equals the value of a constant obtained from a fit to the time integral of the time correlation function in the same interval. Thus, diffusion coefficients could have equally well been evaluated from time correlation functions [29].

**Table 1. Intermolecular potential parameters and charge**

| Molecule | | $\sigma$[Å] | $\varepsilon$[K] | q [e] |
|---|---|---|---|---|
| Carbon dioxide [22] | C-C | 3.033 | 28.129 | +0.6512 |
| | O-O | 2.757 | 80.507 | −0.3256 |
| Naphthalene [18] | C-R1 | 3.695 | 67.229 | 0.0000 |
| | C-R | 3.700 | 41.419 | 0.0000 |
| Dimethylnaphthalene [18] | C_R1 | 3.695 | 69.723 | 0.0000 |
| | C_R | 3.880 | 28.994 | 0.0000 |
| | Si_R | 3.700 | 41.419 | 0.0000 |
| | C_13 | 3.750 | 13.530 | 0.0000 |

In this work, the diffusion coefficients have been calculated between 30 ps and 50 ps by the slope of a mean squared displacement function.

## 3. Gear Predictor-corrector Method

The gear predictor corrector algorithm has been used in simulation which improves efficiency, but the iteration procedure cannot be completely avoided. The gear method is a classical method consisting of the simplest polynomial predictor and a corrector to determine the means of the v(t) and r(t), which are closely dependent on the assumptions made about a(t), and which result in different simulation methods. In gear predictor-corrector algorithms, higher order terms in the Taylor expansion are used to predict steps along the trajectory, and then the actual particle accelerations computed for those points are compared to those that were predicted by the Taylor expansion. The differences between the actual and predicted values are used to correct the position of the point on the trajectory [30-32].

## RESULTS AND DISCUSSION

An NVT ensemble, which is called a canonical ensemble MD simulation, was applied to calculate the diffusion coefficients in super-

**Table 2. The length of a cubic cell used in the simulations**

| v [cm³/mol] | $l$ [Å] |
|---|---|
| 40 | 25.71499249 |
| 50 | 27.70063594 |
| 60 | 29.43631815 |
| 70 | 30.98839511 |
| 80 | 32.39891273 |
| 100 | 34.90061431 |
| 120 | 37.08743687 |
| 150 | 39.95123028 |
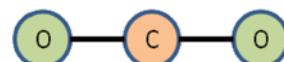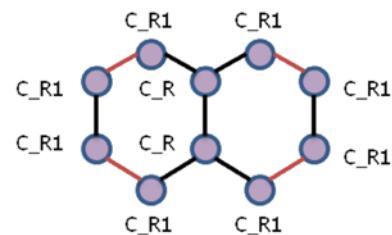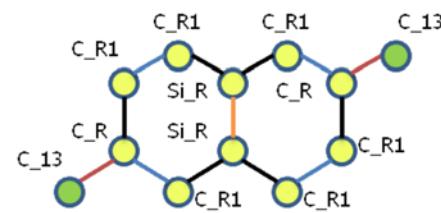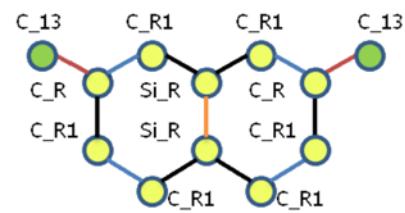


Fig. 1. The structures of carbon dioxide, naphthalene, 2,6-dimethylnaphthalene and 2,7-dimethylnaphthalene used in the molecular simulations.

**Table 3. Calculated results of diffusion coefficients of carbon dioxide, naphthalene, 2,6-dimethylnaphthalene and 2,7-dimethylnaphthalene at 317.5 K**

| Pure carbon dioxide | | | Carbon dioxide (1)+naphthalene (2) | | | |
|---|---|---|---|---|---|---|
| v [cm³/mol] | P [Mpa] | D×10⁸ [m²/s] | v [cm³/mol] | P [Mpa] | D₁×10⁸ [m²/s] | D₂×10⁸ [m²/s] |
| 60 | 13.6490 | 2.279052 | 50 | 17.9697 | 1.511308 | 0.989336 |
| 80 | 11.8077 | 3.455879 | 60 | 15.1892 | 2.132804 | 0.880228 |
| 100 | 10.1289 | 4.471802 | 70 | 12.1696 | 2.846175 | 0.859658 |
| 120 | 9.5759 | 5.628574 | 100 | 10.1125 | 4.411213 | 1.482982 |
| 150 | 8.8549 | 7.120219 | 120 | 9.2321 | 5.711718 | 2.047809 |
| | | | 150 | 8.8965 | 6.927376 | 3.671937 |

| Carbon dioxide (1)+2,6-dimethylnaphthalene (2) | | | | Carbon dioxide (1)+2,7-dimethylnaphthalene (2) | | | |
|---|---|---|---|---|---|---|---|
| v [cm³/mol] | P [Mpa] | D₁×10⁸ [m²/s] | D₂×10⁸ [m²/s] | v [cm³/mol] | P [Mpa] | D₁×10⁸ [m²/s] | D₂×10⁸ [m²/s] |
| 40 | 127.7730 | 0.843399 | 0.301031 | 40 | 123.4786 | 0.863581 | 0.474168 |
| 50 | 19.0592 | 1.526922 | 0.703624 | 50 | 18.8851 | 1.511236 | 1.201598 |
| 60 | 14.9391 | 2.183780 | 1.052775 | 60 | 15.8048 | 2.148198 | 1.698282 |
| 70 | 11.9860 | 1.511236 | 1.201598 | 80 | 10.8928 | 3.447764 | 1.575863 |
| 100 | 8.8498 | 4.424247 | 2.057316 | 100 | 9.9400 | 4.433834 | 1.657225 |
| 150 | | 7.044837 | 3.068370 | 150 | 8.9240 | 7.126000 | 2.536917 |

critical carbon dioxide. The canonical ensemble is a collection of all systems whose thermodynamic state is characterized by a fixed number of atoms, N, a fixed volume, V, and a fixed temperature, T. In this work, the system consists of 256 particles of carbon dioxide for self-diffusion coefficient in a cubic cell with periodic boundary conditions. Each binary system consists of 1 particle of naphthalene, 2,6-dimethylnaphthelene, and 2,7-dimethylnaphthalene, and 255 particles of carbon dioxide. The simulations were performed at an initial temperature of 317.5 K.

For the practical purposes of molecular modeling, it is customary to neglect sufficiently small forces [33]. This is done by setting a distance, called the cutoff distance, at which it is assumed that all direct interactions between one atom and another would involve negligible forces. In this work, to avoid structural artifacts, the cutoff distance was set to half the molecular length. Both the energy and its derivative become zero at these cutoff distances in L-J (12-6) potential function and do not to lead to undesirable discontinuity. In practice, cutoff distances are usually employed in evaluating non-bonded interactions, so the simulation cell needs to be surrounded by only one set of nearest neighbors [31]. The length of a cubic cell used in the simulations is shown in Table 2.

The time step for integration of the equation of motion was set to 1 fs and a production run for a 256 particle system consisting of 1,000,000 time steps to reach equilibrium condition. The time steps should be as large as possible to still get accurate trajectories on the time scale needed and conserve of energy. From the start time 100 steps, a time interval for output 100 steps was determined to prevent wild fluctuations and get efficient conformation samples.

The diffusion coefficients were calculated by the slope of mean square displacements between 30 ps and 50 ps.

All calculations were done using the software WinMASPHYC 2.0 Pro, version number 2.00.015 and WinMASPHYC 2.0 Ultra, version number 2.00.015 to measure diffusion coefficients. The calculated diffusion coefficients of carbon dioxide and aromatic compounds in supercritical carbon dioxide at 317.5 K are shown in Table 3 and Figs. 2-6.

As shown in Fig. 2, the calculated diffusion coefficients for each system behaved as a monotonic decreasing function of the molar density. The simulated results of this work are slightly smaller than the experimental results [15,16], because the approximation of L-J sphere is rough and the diameters of the solute molecules are large. In this study, the molecular simulations data and the selected experimental data show a similar tendency even near the critical point of carbon dioxide. For aromatic compounds, the diffusion coefficients of naphthalene are slightly larger than the ones of 2,6-dimethylnaphthalene and 2,7-dimethylnapathalene, since the side-chain effects of methyl group have occurred between molecules and have affected intermolecular potential parameters.
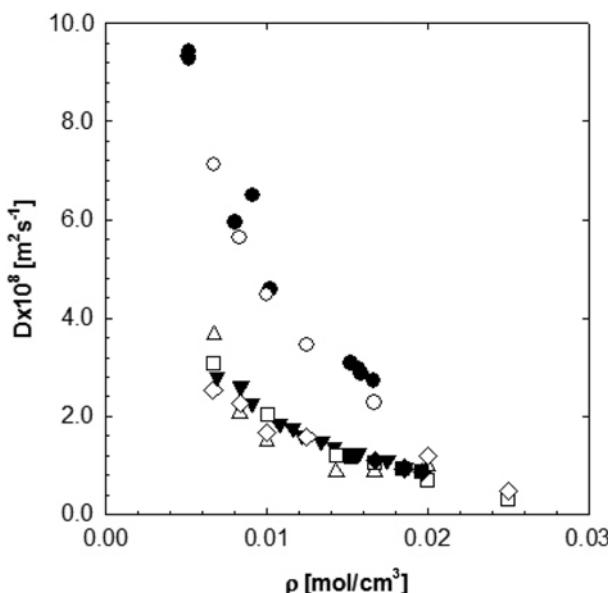


Fig. 2. Diffusion coefficients of carbon dioxide, naphthalene, 2,6-dimethylnaphthalene (2,6DMN) and 2,7-dimethylnaphthalene (2,7DMN) in supercritical carbon dioxide at 317.5 K as function of molar density. Experimental data: ● carbon dioxide in pure carbon dioxide at 308.2 K [35], ▼ naphthalene in carbon dioxide+naphthalene at 318.2 K [5], ■ 2,6-dimethylnaphthalene in carbon dioxide+2,6-dimethylnapahthalene at 308.2 K [16], ◆ 2,7-dimethylnaphthalene in carbon dioxide+2,7-dimethylnapahthalene at 308.2 K [16]. Calculated results at 317.15 K: ○ carbon dioxide in pure carbon dioxide, △ naphthalene in carbon dioxide+naphthalene, □ 2,6-dimethylnapahthalene in carbon dioxide+2,6-dimethylnaphthalene, ◇ 2,7-dimethylnaphthalene in carbon dioxide+2,7-dimethylnapathalene.
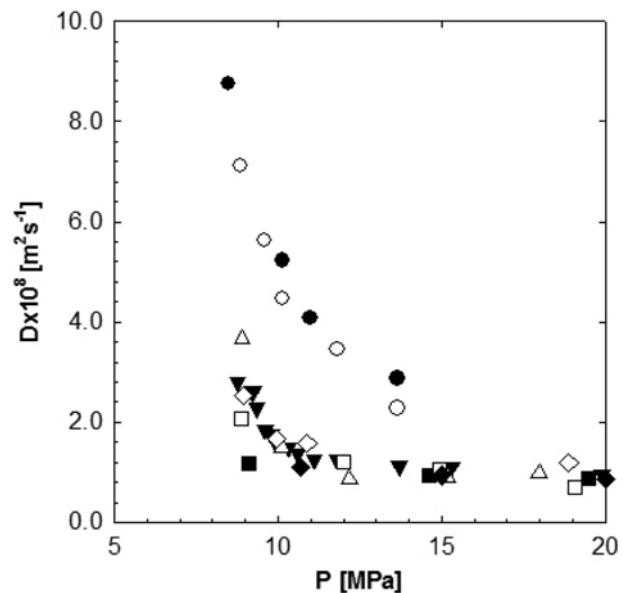


Fig. 3. Diffusion coefficients of carbon dioxide, naphthalene, 2,6-dimethylnaphthalene (2,6DMN) and 2,7-dimethylnaphthalene (2,7DMN) in supercritical carbon dioxide as function of pressure. Experimental data: ● carbon dioxide in pure carbon dioxide at 323.15 K [36], ▼ naphthalene in carbon dioxide+naphthalene at 318.2 K [5], ■ 2,6-dimethylnaphthalene in carbon dioxide+2,6-dimethylnapahthalene at 308.2 K [16], ◆ 2,7-dimethylnaphthalene in carbon dioxide+2,7-dimethylnapahthalene at 308.2 K [16]. Calculated results at 317.15 K: ○ carbon dioxide in pure carbon dioxide, △ naphthalene in carbon dioxide+naphthalene, □ 2,6-dimethylnapahthalene in carbon dioxide+2,6-dimethylnaphthalene, ◇ 2,7-dimethylnaphthalene in carbon dioxide+2,7-dimethylnapathalene.
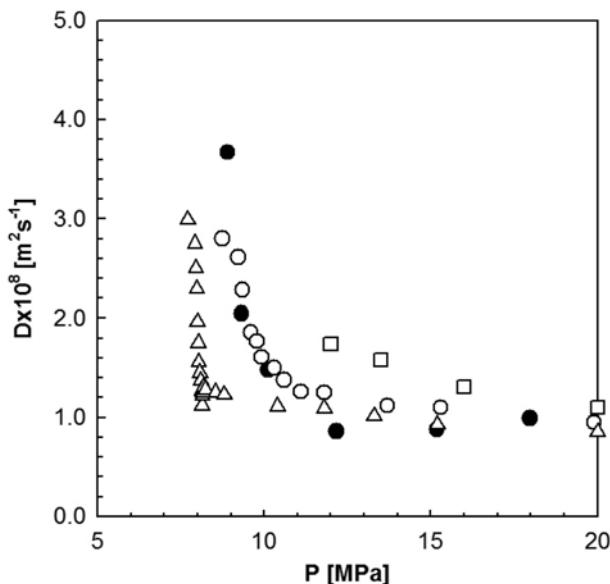
Fig. 4. Diffusion coefficient of naphthalene as function of pressure. Experimental data: ○ naphthalene in carbon dioxide+naphthalene at 318.15 K [5], △ naphthalene in carbon dioxide +naphthalene at 308.2 K [5], □ naphthalene in carbon dioxide+naphthalene at 328.15 K [37]. Calculated results: ● naphthalene in carbon dioxide+naphthalene at 317.15 K.
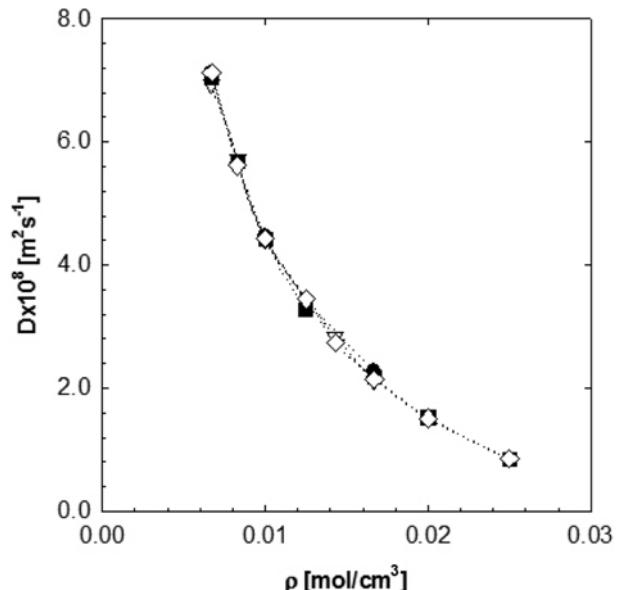


Fig. 6. Diffusion coefficient of supercritical carbon dioxide at 317.5 K as function of molar density. Calculated results at 317.15 K. ● carbon dioxide in pure carbon dioxide, ▽ carbon dioxide in carbon dioxide+naphthalene, ■ carbon dioxide in carbon dioxide+2,6-dimethylnaphthalene, ◇ carbon dioxide in carbon dioxide+2,7-dimethylnaphthalene.
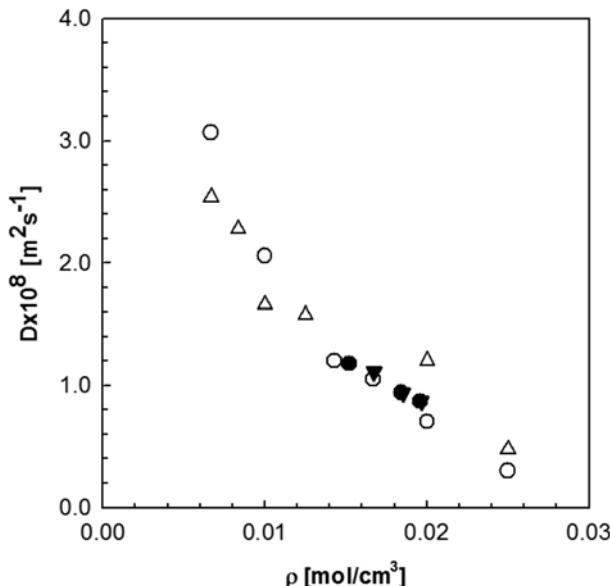


Fig. 5. The molar volume of carbon dioxide, naphthalene, 2,6-dimethylnaphthalene (2,6DMN) and 2,7-dimethylnaphthalene (2,7DMN) in supercritical carbon dioxide as a function of pressure. Experimental data: ● 2,6-dimethylnaphthalene in carbon dioxide+2,6-dimethylnapathalene at 308.2 K [16], ▼ 2,7-dimethylnaphthalene in carbon dioxide+2,7-dimethylnapathalene at 308.2 K [16]. Calculated results at 317.5 K: ○ 2,6-dimethylnaphthalene in carbon dioxide+2,6-dimethylnapathalene, △ 2,7-dimethylnaphthalene in carbon dioxide+2,7-dimethylnapathalene.

Fig. 3 shows the pressure dependence of the diffusion coefficients and Fig. 4 the diffusion coefficients of naphthalene at different tem-

peratures. The difference between calculated values and the experimental ones is sufficiently small. Fig. 3 and Fig. 4 suggest that the diffusion coefficients can be expressed as a function of the pressure at similar temperature. The calculated results of diffusion coefficients are listed in Table 3.

As indicated in Fig. 5, the diffusion coefficients of 2,6-dimethylnaphthalene and 2,7-dimethylnaphthalene are slightly different. One possible explanation is that stacking of molecular arrangements referred to $\pi$-$\pi$ interaction [34] has occurred because overlapping of p-orbital in $\pi$-conjugated system has affected inter-atomic interaction.

Fig. 6 shows the calculated diffusion coefficients of SCCO2 as a decreasing monotonic function of molar density at 317.5 K. The simulation was done by using a periodic boundary condition for a system containing 256 particles. In the case of self-diffusion coefficient all of the particles were carbon dioxide molecules. For the binary systems one molecule was set to represent the naphthalene molecule, and the remaining 255 particles were modeled as carbon dioxide molecules. The absolute difference in CO2 molecules for the two cases is just a single molecule, which explains the similar behavior of the diffusion coefficients obtained by the simulations.

## CONCLUSIONS

The molecular dynamics simulation using gear predictor corrector algorithm has shown to be proven acceptable in predicting diffusion coefficients of carbon dioxide, naphthalene, 2,6-dimethylnaphthalene, and 2,7-dimethylnaphthalene in SCCO2 system.

The calculated diffusion coefficients with Lennard-Jones (12-6) and Coulomb potential functions when compared with the experimental ones and show a similar tendency near the critical point. There-

fore, the authors believe that suggested procedure has proven the reliability of molecular simulation for the prediction high-pressure diffusion coefficients for the selected mixtures.

The simulation accuracy might be improved if the pressure would be averaged over a larger number of simulation time steps. However, this would increase the simulation time considerably, thus making it more inefficient as engineering tool. An optimum would be a balance between simulation time and pressure deviation, and the authors believe that the presented results are close to the optimum.

## REFERENCES

1. N. Koichiro, *Fluid Phase Equilib.*, **144**, 217 (1998).
2. Y. V. Tsekhanskaya, M. B. Iomtev and E. V. Mushkina, *Russ. J. Phys. Chem.*, **38**, 1173 (1996).
3. H. Nichiumi, M. Fujita and K. Agou, *Fluid Phase Equilib.*, **117**, 356 (1996).
4. K. Ago and H. Nishiumi, *Ind. Eng. Chem. Res.*, **37**, 1692 (1998).
5. H. Higashi, Y. Iwai, Y. Nakamura, S. Yamamoto and Y. Arai, *Fluid Phase Equilib.*, **166**, 101 (1999).
6. M. Fermeglia and S. Pricl, *Fluid Phase Equilib.*, **166**, 21 (1999).
7. E. Kiran and J. F. Brennecke, *Supercritical fluid engineering science*, American Chemical Society Symposium Series, Los Angeles (1991).
8. J. L. Bueno, J. J. Suarez, J. Dizy and I. Medina, *J. Chem. Eng.*, **38**, 344 (1998).
9. A. E. Nasrabad, *J. Chem. Phys.*, **130**, 024503 (2009).
10. A. P. Eaton and A. Akgerman, *Ind. Eng. Chem. Res.*, **36**, 923 (1997).
11. W. H. Xu, J. C. Yang and Y. Y. Hu, *J. Phys. Chem. B.*, **113**, 4781 (2009).
12. M. Fermeglia and S. Pricl, *AIChE J.*, **45**, 2619 (1999).
13. H. Higashi, Y. Iwai and Y. Arai, *Ind. Eng. Chem. Res.*, **39**, 4567 (2000).
14. H. Higashi, Y. Iwai, H. Uchida and Y. Arai, *J. Supercrit. Fluids*, **13**, 93 (1998).
15. H. Higashi, Y. Iwai and Y. Arai, *Fluid Phase Equilib.*, **234**, 51 (2005).
16. H. Higashi, Y. Iwai, Y. Takahashi, H. Uchida and Y. Arai, *Fluid Phase Equilib.*, **144**, 269 (1998).
17. G. Raabe, B. D. Todd and R. J. Sadus, *J. Chem. Phys.*, **123**, 034511 (2005).
18. D. W. Collin, G. M. Marcus and J. I. Siepmann, *J. Phys. Chem. B.*, **104**, 8008 (2000).
19. J. Vorholz, V. I. Harismiadis, B. Rumpf, A. Z. Panagiotopoulos and G. Maurer, *Fluid Phase Equilib.*, **170**, 203 (2000).
20. A. Srivastava, C. Alleman, S. Ghosh and L. J. Lee, *Modelling Simul. Mater. Sci. Eng.*, **18**, 22 (2010).
21. Y. Iwai, H. Uchida, Y. Koga and Y. Arai, *Ind. Eng. Chem. Res.*, **35**, 3782 (1996).
22. J. G. Harris and K. H. Yung, *J. Phys. Chem.*, **99**, 12021 (1995).
23. J. J. Potoff, J. R. Errington and A. Z. Panagiotopoulos, *Mol. Phys.*, **97**, 1073 (1999).
24. H. Higashi, Y. Iwai and Y. Arai, *Chem. Eng. Sci.*, **56**, 3027 (2001).
25. A. White, *DSTO aeronautical and maritime research laboratory*, Melbourne (2000).
26. K. Meier, *Computer simulation and interpretation of the transport coefficients of the lennard-jones model fluid*, Dissertation, University of the Federal Armed Forces Hamburg (2002).
27. N. Attig, K. Binder, H. Grubmueller and K. Kremer, *NIC Series*, **23**, 1 (2004).
28. M. P. Allen and D. J. Tildesley, *Computer simulation of liquids*, Clarendon Press, Oxford (1987).
29. K. Meier, A. Laesecke and S. Kabelac, *Int. J. Thermodynam.*, **22**, 161 (2001).
30. J. Kolafa, *J. Chem. Phys.*, **122**, 164105 (2005).
31. C. J. Cramer, *Essentials of computational chemistry*, John Wiley & Sons, Ltd., West Sussex (2004).
32. L. J. Hou and Z. L. Miskovic, *Comput. Phys.*, arXiv:0806. 3912v2 (2008).
33. W. Ware, *Distributed molecular modeling over very-low-bandwidth computer networks*, The Fifth Foresight Conference on Molecular Nanotechnology (1997).
34. G. B. McGaughey, M. Gagne and A. K. Rappe, *J. Biological Chem.*, **273**, 15458 (1998).
35. H. A. Jr. O'hern and J. J. Martin, *Ind. Eng. Chem.*, **47**, 2081 (1955).
36. P. Etesse, J. A. Zega and R. Kobayashi, *J. Chem. Phys.*, **97**, 2022 (1992).
37. D. M. Lamb, S. T. Adamy, K. W. Woo and J. Jonas, *J. Phys. Chem.*, **93**, 5002 (1989).